

## NUMERICAL STUDY ON STABILITY FOR TSUNAMI AND EARTHQUAKE OF THE TSUNAMI EVACUATION BUILDING WITH PILOTI

YUKI OHKI<sup>1</sup>, TARO ARIKAWA<sup>2</sup>

*1 Chuo university, Japan, a12.he8n@g.chuo-u.ac.jp*

*2 Chuo university, Japan, arikawa@civil.chuo-u.ac.jp*

### ABSTRACT

Tsunami evacuation building acts as an emergency place when people can't reach to the safety area. In these days, the piloti construction may be suitable as tsunami evacuation building in terms of reduction of tsunami force. However, such building is vulnerable to an earthquake motion, and the damage may be caused by the strong earthquake vibration. But there are any estimation method to confirm the stability for the superposition phenomena. Therefore, in this study the validity of numerical simulations are verified by comparison with the physical model to develop the estimation tools for such kind of phenomena.

CADMAS-STR( Arikawa et al, 2011) was used as the numerical simulators. This simulator is consist of two solver, fluid analysis and structure analysis. The fluid analysis is based on the CADMAS-SURF/3D(Arikawa et. al.,2005), which is 3D NS equation with VOF. The structural part is analyzed by using FEM. By using this coupling method, we compared with the physical model tests(Arikawa et. al., 2016). As the calculation conditions, levels of earthquake vibration and 1 solitary wave were used. At first, without vibration condition is compared, and next the solitary wave attacks after vibrations. This building was made of concrete and was connected with the floor by a reinforcing bar.

**KEYWORDS:** tsunami evacuation building, piloti, stability, earthquake, CADMAS-STR/3D

### 1 INTRODUCTION

As a result of the tsunami whose scale was far in excess of assumptions, generated by the March 11, 2011, Tohoku district Pacific Offing Earthquake, Japan suffered catastrophic damage. The way of thinking about the form of tsunami-disaster mitigation has changed since and, to mitigate earthquake disasters, thinking is shifting from a line of defense by simple breakwater structures to defense not only breakwaters but on their use alongside municipal facilities, as well.

The improvement of tsunami-refuge facilities such as a tsunami-refuge buildings or tsunami-refuge towers is advancing into the areas where tsunami damage is predicted in the future should a Nankai-trough earthquake occur. Although the aforementioned structures use materials-that are designed to have strong proof stress against tsunami, the examination of earthquake power is still insufficient and weak for earthquake-proofing, and so these structures may not demonstrate a seaworthiness ability at the time of a tsunami attack.

In this study, I examined the safety evaluation for an earthquake, and refuge building at the same time with the aim of establishing a numerical computation technique for an earthquake, the tsunami using calculation system CADMAS-STR3D (Arikawa et al., 2012) calculation system which enabled fluid and coupling analysis of the structure.

### 2 METHOD OF ANALYSIS

#### 2.1 SUMMARY OF CADMAS-SURF/3D

Numerical value wave waterway CADMAS-SURF/3D (Arikawa et al., 2007) is a numerical value model developed for the purpose of applying to the business of the wave design of sea area facilities-resistant. (research and development p6 12,3 of the numerical value wave waterway) use the expression that a shape was similar to by a Paula model by consecutive expressions and the Navier-Stokes equation of the incompressible viscous fluid as a basic equation, and break up, and use the Euler method and the SMAC method technique. Specifically, see the research and development of the numerical value wave waterway of references for specifics .

### 2.1.1 Basic Equation

$$\frac{\partial \gamma_x u}{\partial x} + \frac{\partial \gamma_y v}{\partial y} + \frac{\partial \gamma_z w}{\partial z} = S_p \quad (1)$$

$$\lambda_v \frac{\partial u}{\partial t} + \frac{\partial \lambda_x uu}{\partial x} + \frac{\partial \lambda_y uv}{\partial y} + \frac{\partial \lambda_z uw}{\partial z} = -\frac{\gamma_v}{\rho} \frac{\partial P}{\partial x} + \frac{\partial}{\partial x} \left\{ \gamma_x v_e \left( 2 \frac{\partial u}{\partial x} \right) \right\} + \frac{\partial}{\partial y} \left\{ \gamma_y v_e \left( \frac{\partial u}{\partial y} + \frac{\partial v}{\partial x} \right) \right\} + \frac{\partial}{\partial z} \left\{ \gamma_z v_e \left( \frac{\partial u}{\partial z} + \frac{\partial w}{\partial x} \right) \right\} - D_x u + S_u - R_x \quad (2)$$

$$\lambda_v \frac{\partial v}{\partial t} + \frac{\partial \lambda_x vu}{\partial x} + \frac{\partial \lambda_y vv}{\partial y} + \frac{\partial \lambda_z vw}{\partial z} = -\frac{\gamma_v}{\rho} \frac{\partial P}{\partial y} + \frac{\partial}{\partial x} \left\{ \gamma_x v_e \left( \frac{\partial v}{\partial x} + \frac{\partial u}{\partial y} \right) \right\} + \frac{\partial}{\partial y} \left\{ \gamma_y v_e \left( 2 \frac{\partial v}{\partial y} \right) \right\} + \frac{\partial}{\partial z} \left\{ \gamma_z v_e \left( \frac{\partial v}{\partial z} + \frac{\partial w}{\partial y} \right) \right\} - D_y v + S_v - R_y \quad (3)$$

$$\lambda_v \frac{\partial w}{\partial t} + \frac{\partial \lambda_x wu}{\partial x} + \frac{\partial \lambda_y wv}{\partial y} + \frac{\partial \lambda_z ww}{\partial z} = -\frac{\gamma_v}{\rho} \frac{\partial P}{\partial z} + \frac{\partial}{\partial x} \left\{ \gamma_x v_e \left( \frac{\partial w}{\partial x} + \frac{\partial u}{\partial z} \right) \right\} + \frac{\partial}{\partial y} \left\{ \gamma_y v_e \left( \frac{\partial w}{\partial y} + \frac{\partial v}{\partial z} \right) \right\} + \frac{\partial}{\partial z} \left\{ \gamma_z v_e \left( 2 \frac{\partial w}{\partial z} \right) \right\} - D_z w + S_w - R_z - \gamma_v g \quad (4)$$

$\lambda_v, \lambda_x, \lambda_y, \lambda_z$  is expressed as follows if I assume it an inertial force coefficient, and it is with the effect of the inertial force that right side Clause 2 receives from a structure.

$$\begin{cases} \lambda_v = \gamma_v + (1 - \gamma_v) C_M \\ \lambda_x = \gamma_x + (1 - \gamma_x) C_M \\ \lambda_y = \gamma_y + (1 - \gamma_y) C_M \\ \lambda_z = \gamma_z + (1 - \gamma_z) C_M \end{cases} \quad (5)$$

$C_D$  modeled resistance  $R_x, R_y, R_z$  from many apertures quality in form in proportion to square of the speed as coefficient of drag as follows

$$R_x = \frac{1}{2} \frac{C_D}{\Delta x} (1 - \gamma_x) u \sqrt{u^2 + v^2 + w^2} \quad (6)$$

$$R_y = \frac{1}{2} \frac{C_D}{\Delta y} (1 - \gamma_y) v \sqrt{u^2 + v^2 + w^2} \quad (7)$$

$$R_z = \frac{1}{2} \frac{C_D}{\Delta z} (1 - \gamma_z) w \sqrt{u^2 + v^2 + w^2} \quad (8)$$

### 2.1.2 FREE WIND DRIFT ANALYSIS MODEL

Versatility was high and, in a free surface analysis model, adopted the VOF (Volume of Fluid) method which could analyze a complicated surface shape

$$\gamma_v \frac{\partial F}{\partial t} + \frac{\partial \gamma_x u F}{\partial x} + \frac{\partial \gamma_y v F}{\partial y} + \frac{\partial \gamma_z w F}{\partial z} = S_F \quad (9)$$

We make the advection equation mentioned above disintegration by the donor lye septa method which increased improvement.

With the VOF method which increased improvement for free surface analysis; using the studio guard mesh spatial; break up, and become disintegration by technique.

### 2.1.3 BOUNDARY CONDITION

I set an emission border of Sommerfeld to show for boundary condition as follows.

$$\frac{\partial f}{\partial t} + C \frac{\partial f}{\partial t} = 0 \quad (9)$$

### 2.1.4 ENERGY DECREMENT ZONE

I used the following two sets as an energy decrement zone in the numerical value wave waterway.

$$D_x = \theta_x \sqrt{\frac{g}{h}} (N + 1) \left( \frac{x - x_0}{l} \right)^N \quad (10)$$

$$D_y = \theta_y \sqrt{\frac{g}{h}} (N + 1) \left( \frac{x-x_0}{l} \right)^N \quad (11)$$

$$D_z = \theta_z \sqrt{\frac{g}{h}} (N + 1) \left( \frac{x-x_0}{l} \right)^N \quad (12)$$

I performed wave-making by data.mtb with the matrix data file about wave-making of the soliton and show it as follows

$$\eta(x, t) = H \operatorname{sech}^2\{k(x - Ct)\} \quad (13)$$

We used it and calculated the speed in each point in time, quantity of water level change and give speed provided on an analysis domain boundary surface based on the wave-making water level change quantity.

## 2.2 SUMMARY OF CADMAS-STR/3D

CADMAS-STR3D (Arikawa et al., 2012) is the structure fluid calculation system which enabled coupling -with Femap which is CADMAS-SURF3D and the structural calculation system mentioned above. I calculate displacement for the cause by the pressure that pressure could calculate in the CADMAS side, as shown in Figure -1, and enabled structural calculation and coupling analysis of the fluid calculation by both sides changing data.

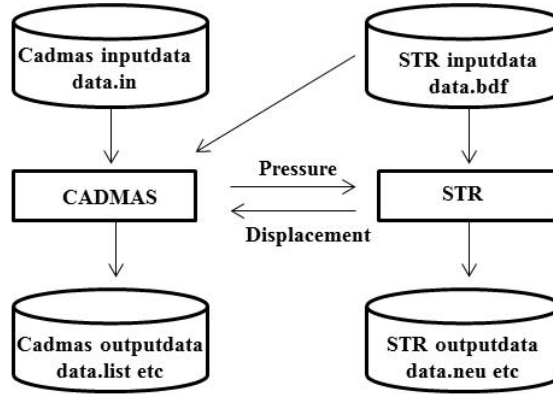


Figure 1. Scheme of coupling analysis for CADMAS-STR/3D

The fluid side expresses the obstacle not to completely bury a cell in although we use a structure lattice by porosity. The porosity changes in terms of time. A continuous exercise equation is just as we showed it by a summary of CADMAS-SURF/3D.

It is expressed by the equilibrium equation such as the next expression when we express an exercise equation when dynamic external force acts on a structure using a stress tensor.

$$\rho_s \frac{\partial^2 u_{si}}{\partial t^2} = \sigma_{ij,j} + \rho_s \ddot{a} \quad (14)$$

When I use appropriate boundary condition for an upper expression and lead an exercise equation by virtual displacement

$$M\ddot{u} + C\dot{u} + Ku = f_s \quad (15)$$

We become disintegration using a finite element method about the structure, and it is necessary to do it to an individual depending on the phenomenon that is physical at the interval for development every independent calculation time at calculation time of CADMAS-SURF/3D and FEM/3D using the Newmark $\beta$  method at time. Therefore, the time of the partner was the same as one's time or performed only the reception to the state that we advanced to earlier and interpolated a state at the existing time of oneself when it was the same or advanced earlier and, in a timing of the transmission and reception of both, calculated the next step.

When the porosity in fluid cell  $\rightarrow$  obstacle cell or obstacle cell  $\rightarrow$  fluid cell and a case to change and the fluid cell suddenly changes a cell by a calculation of the fluid side when I went fluid and coupling analysis of the structure using this calculation technique, big spikes-formed pressure may occur. This cause is that item is included in Poisson equation derived from consecutive expressions and exercise equations at time.

Therefore, I decided to average the amount of change of the porosity with the sub-loop every-thing and step to express the volume of the structure included in the cell every step exactly at time.

### 3 RESULTS AND DISCUSSION

#### 3.1 SUMMARY OF EXPERIMENT

We used the result of a large-scale experiment performed as a calculation object in the Port and Harbor Research Institute on calculating the reproduction of an earthquake, the tsunami by CADMAS-STR/3D.

We installed wave height 14 in total, current meter 4, pressure gauge 20 as an observation point and established the decrement zone in the outflow border part. We performed wave-making -using a wave-making plate, and wave-making soliton. We installed a vibration stand under the model of the refuge building and reproduced earthquake vibrations

We performed the case which produced case, first case, earthquake to produce only the second case, tsunami which produced only third case, earthquake to consider the influence on tsunami refuge building which an earthquake-, and a tsunami had on an experimental case-, for both tsunamis.

#### 3.2 THE CASE OF CADMAS-SURF/3D

##### 3.2.1 WAVE HEIGHT

I went wave-making of the soliton using the matrix data file which I made. I made the structure which I modeled, the experiment waterway together as obstacle, and the transformation by the action wave pressure does not consider it. It was harbor Airport Institute to show on the top (Germany) and compared two of a laboratory finding and the reproduction calculation result by CADMAS-SURF/3D carried out. The waveform can almost reappear in initial wave height, both wave height when it is braking wave observation points. However, the water level drop after the peak is a calculated value more than the laboratory finding it follows, and a dilatational wave after the tsunami action cannot reappear. These two influence the wave that it was done wave-making because, besides, we do not establish the decrement domain on the bank side in the modeling of the experiment waterway that the behavior when this is related to the method of wave-making, and wave-making of the wave by matrix data reproduces only wave-making caused by the anaseism, and wave-making moves to the offing side does not reproduce it reflects it is thought about. Because it is thought that the influence that a dilatational wave gives to a structure is small, in this study, we considered this error as being negligible.

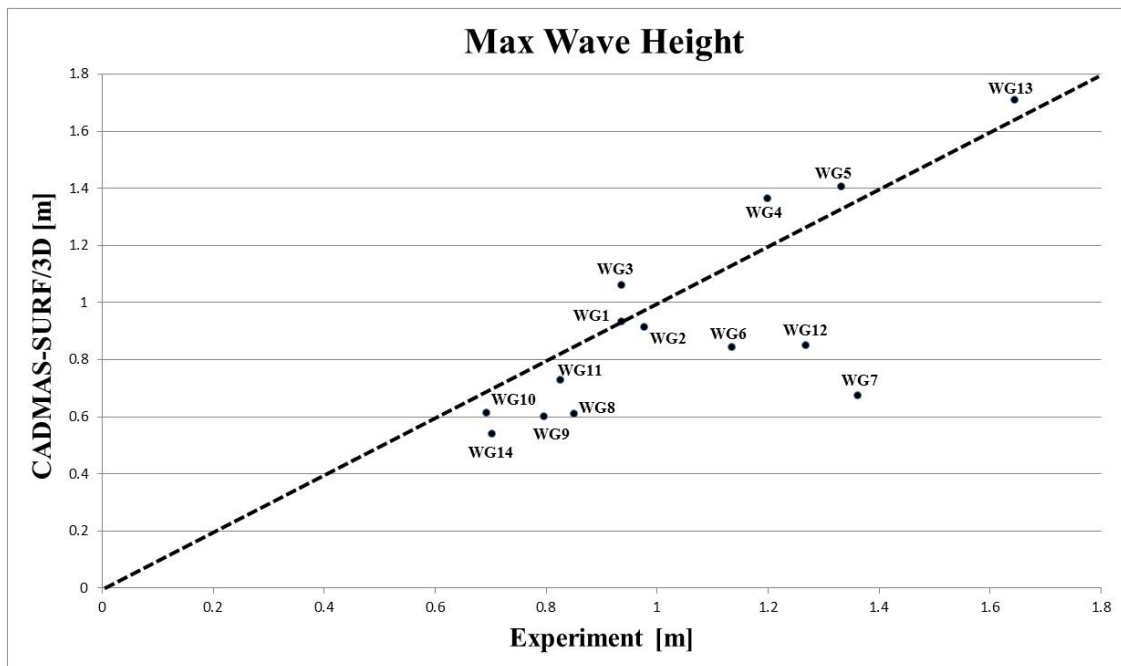


Figure 2. Over-all comparison of the biggest wave height observation point with the laboratory finding

The biggest wave height of all wave height observation points was compared with the laboratory finding by a calculation result to show on Figure-2. In this experiment, the breaking wave occurs before a tsunami collides with a refuge building, and the size of the error is different in the graph mentioned above when it is breaking water.

### 3.2.2 WAVE PRESSURE

We compared the calculation result by CADMAS-SURF/3D with the laboratory finding. A wave pattern, the highest score almost agrees together, but a time gap occurs.

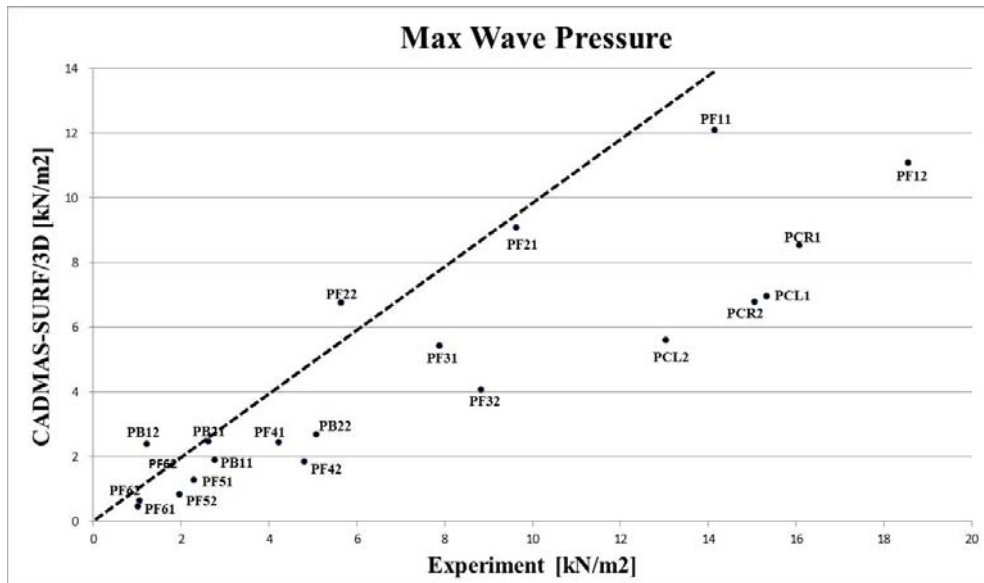


Figure 3. Comparison of the greatest wave pressure

The calculation result by CADMAS-SURF/3D was compared with the laboratory finding is shown in Figure-3. It is different from a laboratory finding in a much observed point. Shock wave pressure-like peak wave pressure produces this in a much -observed point including PF11, and it is thought that this is because the shock wave pressure cannot reappear.

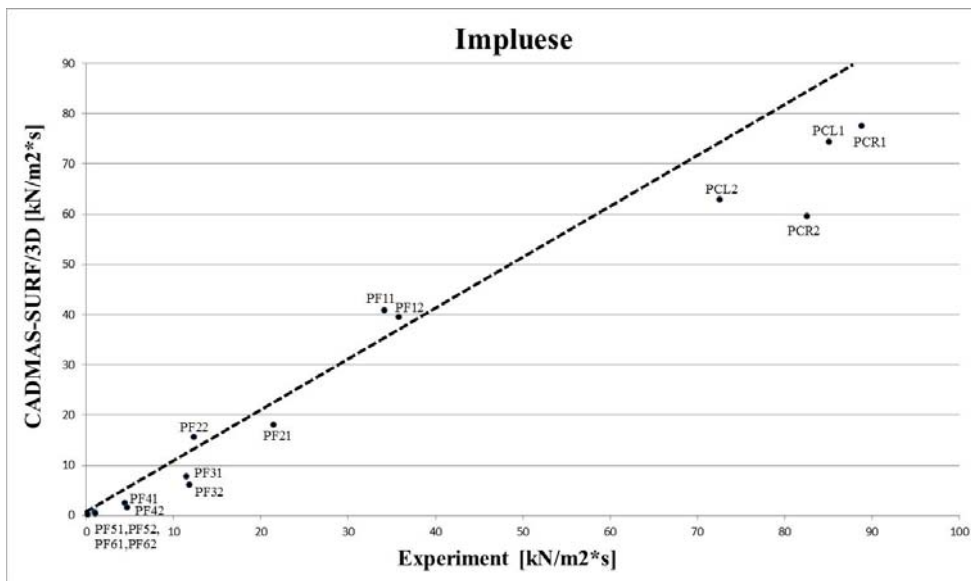


Figure 4. Comparison of impulse with the experimental value

The impulse in each observation point was compared with the laboratory finding by a calculation result by CADMAS-SURF/3D to show in Figure-4. From this graph, we accord with a laboratory finding with the precision that is better than most big wave pressure. Because the wave pattern in each observation point almost accords and agrees on the precision that you may put in the impulse, it may be said that we can reproduce the physical phenomenon of the experiment for action resultant enough because I can reproduce continuous wave pressure to occur for a long time in this study even if we were unable to reproduce enough peak wave pressure occurring in a short time such as the shock wave pressure.

As for the tsunami external force acting on a structure having a piloti form targeted for modeling in this article from the CADMAS-SURF/3D result mentioned above, numerical analysis by CADMAS-SURF/3D revealed that sufficient plasticity was produced in the wave-making method using the matrix data file.

### 3.3 THE CASE OF CADMAS-STR/3D

We modeled a structure by Femap, and the reproduction calculation by CADMAS-STR3D reappeared and was calculated. The properties of matter level calculated density from gross weight and set properties of matter level. CADMAS-STR/3D is two levels of models about the water and air than CADMAS-SURF3D which was a single-layered model. We modeled only the structure on the experiment waterway in Femap and allowed you to consider transformation.

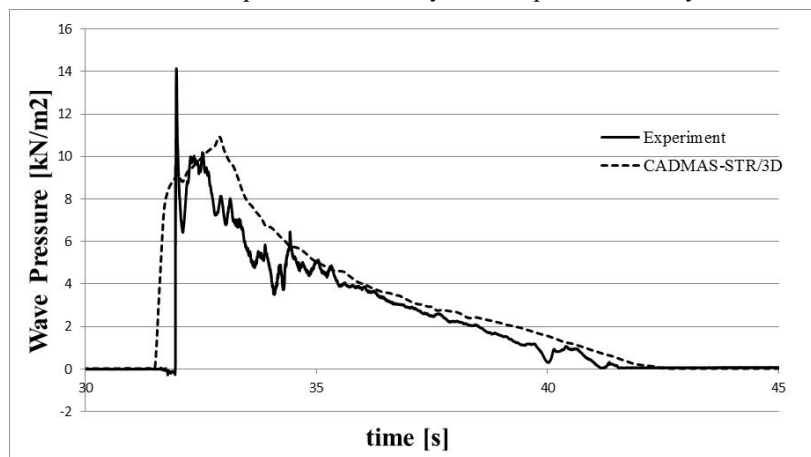


Figure 5. Comparison of observation point PF11 with the experimental value

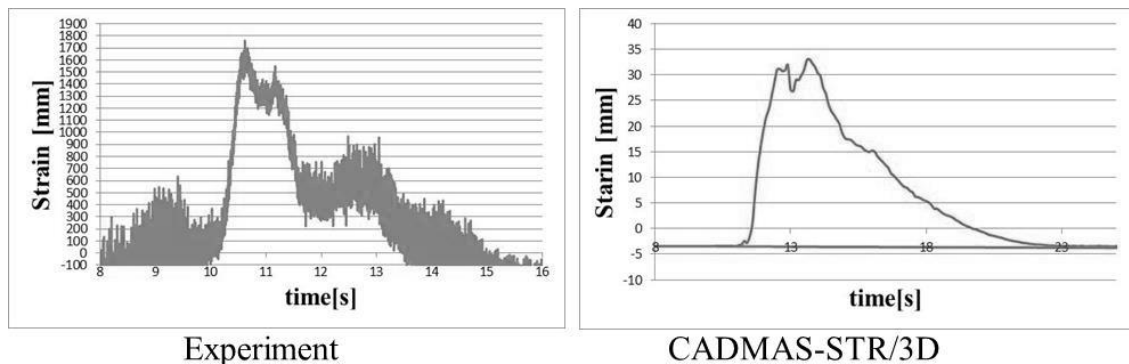


Figure 6. Comparison between experimental value and calculated value SF1

This calculation result was compared with the laboratory finding in observation point PF11, shown in Figure-5, but agrees on the precision that is good for most large wave pressure, wave patterns by a laboratory finding.

Action wave pressure after the peak wave pressure is big and appears at most points of the wave pressure observation point of CADMAS-STR3D, and continuous wave pressure takes the value bigger than the calculation result. This is an error that occurs in coupling analysis of CADMAS-STR/3D. I go through it without the element of the coupling analysis such as the structure being recognized with a simple cavity, and a fluid remaining in the anterior surface of structure when the element of the structure which I modeled by FEM3D is located in the inside of the CADMAS lattice. It is thereby thought that continuous wave pressure after the peak wave pressure is greatly pronounced.

In addition, the calculation result that was provided by CADMAS-STR/3D whereas a result in CADMAS-SURF/3D was able to express wave pattern can reproduce the highest score with good precision about some observation point. It is expected in the future when a good calculation result of the precision is provided by setting the lattice size of the CADMAS side and lattice size of the FEM side well. A comparison of displacement data in observation point SF1 is shown in Figure-6. The wave pattern accords analogously, but in total is almost different. On the occasion of the modeling in the main subject, the density of the structure is calculated from gross weight, and the Young's modulus adopts the maximum of the object of the component of each refuge building. Modeling of this structure in CADMAS-STR3D in the main subject is the numerical

computation that I carried out to examine the plasticity of the experiment with two levels of mind liquid. The displacement expected is not provided without reproducing the first case, hollow structure, and second case, steel reinforced concrete structure that is the characteristic of the refuge building. It is possible to say that the reproduction of the earthquake vibration phenomenon in CADMAS-STR/3D, to be mentioned later, but inside of the reinforcing rod, plays an important role in a structure having a piloti form, and it may be said that examination will be a necessary in the future.

#### 4 EXAMINATION OF AN EARTHQUAKE, A TSUNAMI

##### 4.1 EXAMINATION OF THE SEAWORTHINESS ABILITY IN THE STEEL REINFORCED CONCRETE CONSTRUCTION STRUCTURE

Many structures were carried away or damaged in the Tohoku earthquake disaster. Many of these were not steel-reinforced concrete structures. Consideration of the internal reinforcing rod such as the structures of the steel-reinforced concrete construction is an important issue in the wave design in land structure-resistance. The internal reinforcing rod can reappear by burying it in solid elements as a line element and, in numerical analysis in CADMAS-STR3D, can observe the behavior of a steel reinforced concrete construction structure of fluids.

Therefore I compare case including the internal reinforcing rod and two when I do not include it in a caisson of fluids in this chapter and consider the influence that the inside reinforcing rod of the structure gives the wave force of the structure-resistance.

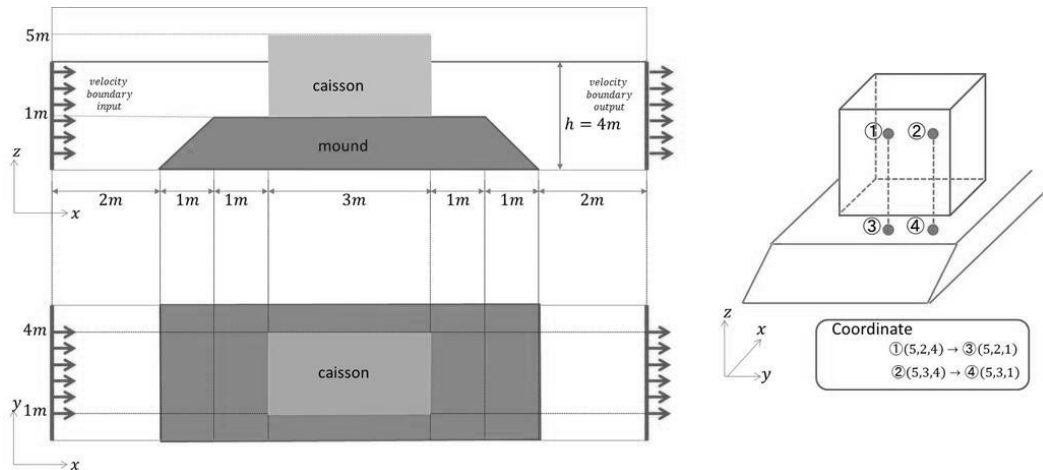
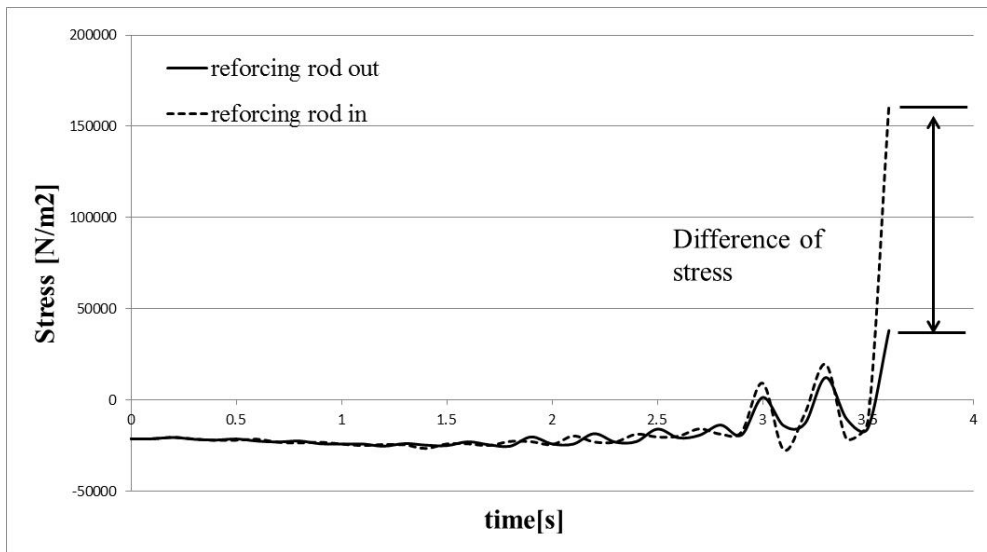


Figure 7. Modeling summary and figure of internal reinforcing rod placement

We assume a waterway as shown in Figure-7 as modeling, and the speed establishes an outflow, the inflow border in two boundary surfaces each. We made the model of two without the first case, inside reinforcing rod to less locate model and the inside reinforcing rod which there was the second case, inside reinforcing rod which placed an internal reinforcing rod like a figure in and flowed out and compared the slide quantity of the caisson by the flow quantity increase as 2m per second in the speed in the inflow border. In addition, it is assumed that one side of the shape of the internal reinforcing rod is a square section of 0.01m, and a caisson, the properties of matter level of the mound are streets in following Table-1.

	density (kg/m <sup>3</sup> )	Young's modulus	Porosity
caisson	1900	2.00E+10	
mound	1900	2.00E+10	0.5
steel	2700	2.00E+11	

Table 1. Properties of material level of each material



**Figure 8. Difference in z direction stress by having inside reinforcing rod or not**

The z direction stress of the caisson in each time is shown in Figure-8. When there is not an internal reinforcing rod, only horizontal power appears, and the caisson does slide as a slide form of the caissons horizontally. They faces each other, and, as for the case including the internal reinforcing rod, it is thought that bending the inside reinforcing rod placement position as an initial point, and the power of the direction acts without doing slide, unlike the case not including horizontally.

The-start time greatly changed on the occasion of having a beam model or not about the slide start time of the caisson. Strength is increased by installing an internal reinforcing rod, and slide time is prolonged and can withstand the tsunami load to for a long time. I understood that I could consider an internal reinforcing rod from a result of this numerical computation in CADMAS-STR/3D.

#### 4.2 EXAMINATION ABOUT THE EARTHQUAKE VIBRATION

Because I examined a transformation reply of the piloti structure for the phenomenon of neither earthquake-, nor tsunami in an experiment in the Port and Airport Research institute where it was said that it was targeted for a reproduction calculation (Germany), there was the result of an earthquake, the tsunami reply, but modeled it separately from an experiment because modeling of a steel reinforced concrete construction structure was difficult. I assumed a structure like the experiment structure, and the properties of matter level modeled it as the concrete piloti structure which did not consider an internal reinforcing rod. The reproduction of the earthquake vibration in CADMAS-STR/3D will give forced displacement in a refuge building base. Vibration should be produced from the ground, but an earthquake wave by the influence such as ground properties amplifies it when I produce earthquake vibration from the ground or might originally do a phenomenon. It was said that it was difficult to consider vibration properties of the ground in CADMAS-STR/3D in the present conditions and aimed at the reproduction of the earthquake vibration in CADMAS-STR/3D in this chapter and I took the action position optionally and considered and examined the result.

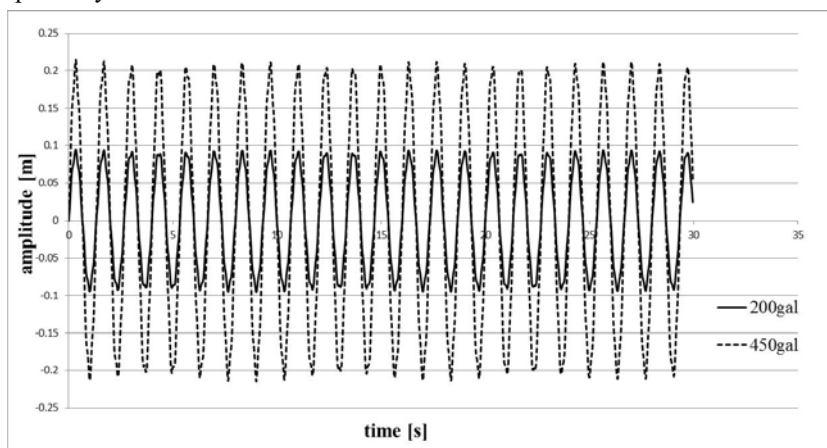


**Figure 9. Action wave pattern**

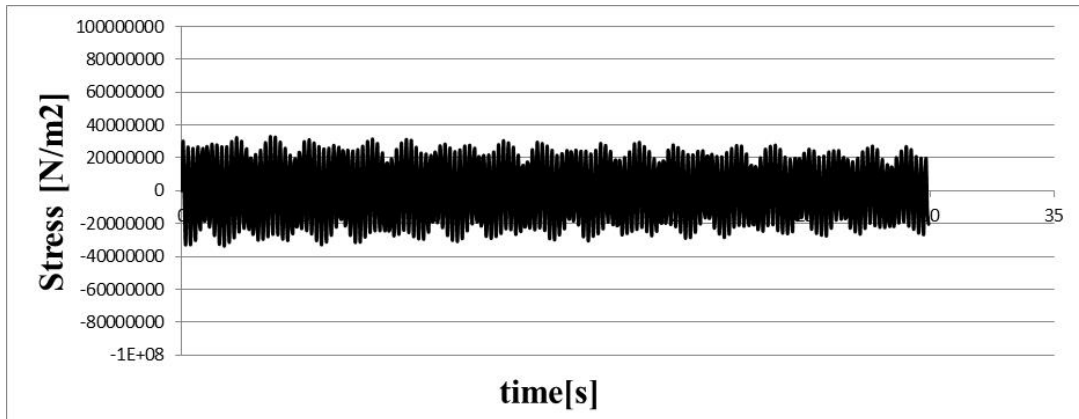


Figure 10. Earthquake load small earthquake (200gal)

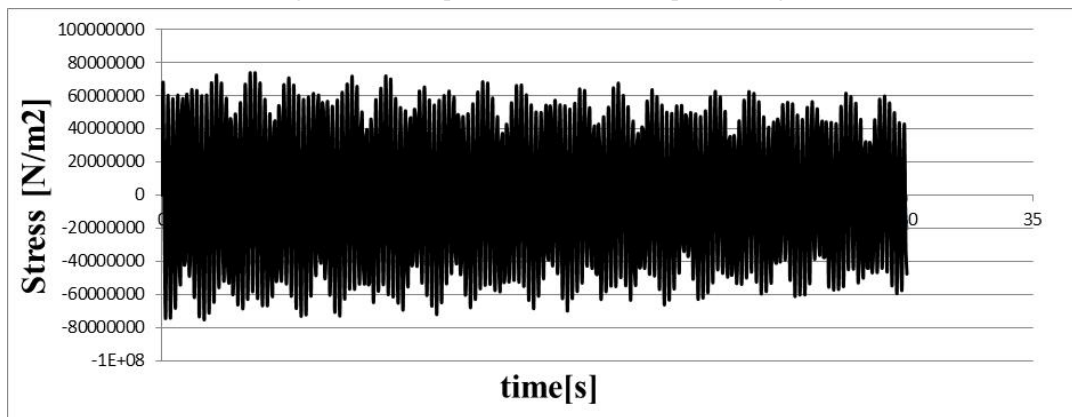


Figure 11. Earthquake load major earthquake (450gal)

The earthquake wave pattern used in this examination to show in Figure-9; first case, small earthquake (200gal), second case, major earthquake (450gal). I changed the number of gals by changing the amplitude in the same period. The earthquake vibration displacement in measurement point SF1 is graphed as shown in Figure-10, 11. The load caused by a major earthquake showed a value larger than that caused by a small earthquake when I compared the two kinds. A big earthquake load occurs in the junction, and it can be understood that enough of the load by the earthquake vibration can reappear.

## 5.CONCLUSION

We performed the consideration with the laboratory finding in a double calculation system of CADMAS-STR/3D which was two levels of mind liquid models with a single-layered model by CADMAS-SURF/3D using free wind-drift analysis by the VOF method coupled with the structural calculation.

In an analysis result in CADMAS-SURF/3D, as for the soliton made coupling in wave-making plate, the plasticity was sufficient to give first case, water level change quantity, second case stability speed, third case, plumb speed in the no level phase that was a matrix data form, the data of three was provided. However, as for the complicated flow under expression and the piloti of the dilatational wave that could not reappear in the method of wave-making of the matrix data form, the result that flow at the refuge building rear became irregular was provided without being able to reproduce it. In addition, there is room for the argument as for the plasticity of breaking water in CADMAS-SURF/3D, and the precision of the wave pattern is big in this study in breaking water and is different.

The result that the shock wave pressure that was the peak wave pressure that occurred in the front wave pressure that was the most dominant pressure in wave pressure to occur in a refuge building in a short time in each measurement point could not be reproduced was provided in the wave pressure. However, I almost agree when I compare the impulse in each wave pressure measurement point, and the continuous wave pressure can reappear sufficient.

Good plasticity is provided about a wave pattern, continuous wave pressure, but plasticity is bad in CADMAS-SURF/3D which is a bed model about the physical phenomenon rolling up the air what's close at hand such as

shock wave pressure or the complicated flow of the structure circumference, and, about the plasticity in CADMAS-SURF/3D, as for the external shock to work to a structure, it is understood that reproduction is difficult by this calculation system. However, the continuous wave pressure that is the dominant wave pressure has sufficient plasticity.

Regarding the result of CADMAS-STR/3D analysis, the peak wave pressure can almost reappear in comparison with the result of CADMAS-SURF/3D calculation of wave pressure provided as a calculation result. However, there are numerous differences in the part of the impulse that lack plasticity. The height of the wave going up the refuge building because of the continuous wave pressure is generally higher than the laboratory finding. In addition, the absolute error of the largest wave pressure grew as the result of CADMAS-SURF/3D calculation so that the plumb height of the observation point became big, and a tendency the same as in the continuous wave pressure to continue was seen.

Many problems remain in reproducing water occurring for a complicated construction such as the piloti structure in a reproduction calculation in CADMAS-STR3D in two levels of mind liquid models that rolled up air, behavior of the air.

## **ACKNOWLEDGEMENT**

This work was supported by Council for Science, Technology and Innovation (CSTI), Cross-ministerial Strategic Innovation Promotion Program (SIP), "Enhancement of societal resiliency against natural disasters" (Funding agency: JST).

## **REFERENCES**

Taro ARIKAWA, Takashi YAMANO, Minoru AKIYAMA, 2007, Advanced Deformation Method for Breaking Waves by using CADMAS-SURF/3D,71-75, PROCEEDINGS OF COASTAL ENGINEERING, JSCE

Taro ARIKAWA, Kazuhiro HAMAGUCHI, Kazushi KITAGAWA, Tomonori SUZUKI, 2010, Development of Numerical Wave Tank Coupled with Structure Analysis Based on FEM, 866-870, PROCEEDINGS OF COASTAL ENGINEERING, JSCE

Daisuke TAKABATAKE, Naoto KIHARA, Nobukazu TANAKA, Numerical Study for the Hydrodynamic Pressure on the Front of Onshore Structures by Tsunami, 851-855, PROCEEDINGS OF COASTAL ENGINEERING, JSCE